acta physica slovaca vol. 56 No. 4, 543 – 553 August 2006

ELECTRON TRANSPORT AT SOLID SURFACES

J. Zemek[1]
Institute of Physics Academy of Sciences of the Czech Republic
Cukrovarnícka 10, 162 53 Prague 6, Czech Republic

Received 23 August 2005, in final form 14 March 2006, accepted 15 March 2006

The common formalism for quantitative analysis in photoelectron spectroscopy and Auger electron spectroscopy is based on the strait-line approximation (SLA) model. Within the SLA, elastic scattering and inelastic surface losses of signal electrons are neglected and ideally flat sample surfaces are assumed. When analyzing real sample surfaces, these assumptions are not usually fulfilled. As a consequence, non-negligible systematic error is introduced into the quantitative results. Based on the present knowledge of electron transport at solid surfaces, influences of electron elastic scattering, electron surface excitation effects, and surface roughness on photoelectron peak areas are reviewed together with the presently developed correcting procedures easy to use in practical surface analysis.

PACS: 68.49.Jk; 79.60.Jv

1 Introduction

The common formalism frequently used in quantitative electron spectroscopy, described by the straight-line approximation (SLA) model [1], assumes a rectilinear motion of signal electrons within a solid. The model is based on several simplifying assumptions:

(i) The studied specimen is polycrystalline or amorphous.

(ii) Electron elastic scattering effects are ignored. As a consequence, the signal electron attenuation in a solid is exponential.

(iii) Surface inelastic excitations of signal electrons are neglected.

(iv) The analyzed solid surface is ideally flat.

Since analyzed solid surfaces are generally complex, covered by overlayers (e.g. oxide layers, surface contaminations) and corrugated, such idealized concept of rectilinear electron motion is only a very rough representation of reality. The above listed assumptions can lead to an overestimation or underestimation of the signal currents of emitted photoelectrons or Auger electrons for particular elements, which in turn will result in a systematic error in quantitative analysis.

[1]E-mail address: zemek@fzu.cz

The first assumption can be easily checked by X-ray or electron diffraction methods, however. Consequences of violation of other assumptions are discussed and illustrated below.

Elastic scattering of signal electrons influences noticeably the measured spectral intensity, as realized previously by Baschenko and Nefedov [2] and others [3–7]. The elastic scattering changes both the initial angular distribution of photoelectrons and the escape probability. Due to complexity of the electron transport, the first attempts to solve the electron transport problem were carried out by Monte Carlo (MC) methods [2, 4, 8–11]. Analytical solutions by solving the Boltzmann kinetic equation in the transport approximation have been also successful [3, 5, 6, 11–13]. MC calculations as well as analytical approaches to the electron transport problem accounting for elastic and inelastic electron scattering processes have shown that the EDDF exhibits generally non-exponential behavior [4, 14, 15]. In particular, it was predicted that in the case of strongly non-isotropic photoelectron emission, the EDDF could reach a maximum at a depth smaller than the corresponding inelastic mean free path (IMFP) [4, 10, 16, 17]. The theoretical predictions have been verified experimentally so far only for several materials: for an aluminum oxide, copper oxide, silver sulphide [10, 12, 16–20] and more recently also for an iron oxide [21].

Surface excitations result from the boundary conditions of the Maxwell equations near the interface between regions with different electrical susceptibility. These modes decay exponentially with the distance from the surface and may be excited by an electron at either side of an interface [22]. Surface excitation effects were underestimated in the past on a base of an idea that the surface and bulk excitation compensates in a near surface region of a solid. More recent results showed [23] that the compensation occurs indeed well beneath the surface while above the surface (in vacuum) the surface excitations are not compensated at all.

The surface electron excitation processes are rather complex. Several models for surface excitations have been proposed [24–30]. The magnitude of the surface excitation probability as well as the distribution of energy losses depend in a complex manner on the direction of surface crossing, the depth below the surface and the energy lost in a surface scattering process. To describe more easily the influence of surface excitations by a single parameter, Chen [31] proposed the surface excitation parameter (SEP).

As mentioned above, quantitative electron spectroscopy is usually applied under an assumption of ideally flat surfaces. It was predicted from model calculations [1, 32] that the angular distribution of peak areas recorded from a homogeneous rough sample is not influenced by the roughness, provided the isotropic emission of signal electrons from their parents atoms. The isotropic emission is expected for Auger emission. Contrary, it is well established that the surface roughness influences strongly number of signal electrons recorded from layered samples, e.g. a thin film grown on a solid surface [1, 33–40]. As a consequence, considerable systematic errors as high as 50% may be introduced when a non-destructive concentration depth profiling or an overlayer thickness is evaluated from the angular-resolved spectra [33–39]. Due to complexity of the quantitative approaches accounting for the effect of real surface roughness, the effect is usually neglected in the evaluation of electron spectra.

There are several attempts in the literature to evaluate the surface roughness effects by a simple regular form of the roughness as triangular or sinusoidal shapes [1, 38, 39]. However, an important step to overcome the general problem of the real surface roughness was taken by Gunter et al. [35, 36]. The authors used a fractal model describing the roughness and studied electron transport by MC calculations. They found that the influence of the surface roughness on photo-

electron spectra is mainly determined by the average steepness of the surface. They also found that for an overlayer/substrate sample the error in an overlayer thickness determination due to the roughness reached a minimum for the so-called magic angle $\sim$35° or $\sim$45° (the emission angle measured from the surface normal), depending on a simple and fully three-dimensional model of a rough surface used, respectively. Vutova et al. [38, 39] analytically calculated the influence of surface roughness (including also the shadowing effect and the photoelectron anisotropy) for the prism-shaped corrugated surface. Werner [32] studied the influence of surface roughness effects (shadowing as well as the true emission angles) on total and angle-dependent signal electron intensities. He incorporated the influence of surface roughness into an effective depth distribution function and found dominating influence of surface roughness over the effect of elastic scattering. The next approach to evaluate the impact of the real sample surface roughness was developed more recently by Chatelier et al. [37]. The authors analyzed rough samples by atomic force microscopy (AFM) to provide a frequency histogram of the local slopes, which is incorporated into the quantitative procedure.

2 Quantitative descriptions and illustrations

To improve and facilitate quantitative analysis in photoelectron spectroscopy, the most important modifications applied to the SLA approach will be outlined on the bases of present understanding of electron transport at solid surfaces. Specifically, the influence of electron elastic scattering effects, the influence of electron motion through a solid surface (electron inelastic surface excitations), and the influence of surface roughness on photoelectron peak areas will be discussed and illustrated.

2.1 Rectilinear motion of signal electrons

Under above mentioned assumptions, the contribution, dI, to the observed signal intensity emitted in the layer of thickness dz at the depth z is given by

$$dI = CI_0AM(d\sigma/d\Omega)c(z)f(E,\alpha)dz, \tag{1}$$

where the constant Ccomprises the instrumental factors, I_0 is the flux of X-rays, A is the analyzed area, M is the atomic density, $c(z)$ is atomic concentration of a given element at a depth z, $f(E,\alpha)$ is the escape probability of electrons with kinetic energy E leaving the solid surface in direction α measured from the surface normal, and $d\sigma/d\Omega$ is the differential photoelectric cross-section [40] derived for unpolarized radiation and random orientation of atoms in a solid,

$$d\sigma/d\Omega = (\sigma_i/4\pi)\{1 - 0.25\beta(3\cos^2\Theta - 1)\}, \tag{2}$$

where $\sigma_i$is the total photoelectric cross-section, β is the asymmetry parameter and Θ is the angle between X-ray propagation direction and direction of emitted electron.

The escape probability, $f(E,\alpha)$, called the emission depth distribution function (EDDF) [41], obeys a simple exponential law within the SLA model. This function describes contributions dI to the total photoelectron current I arising from different depths z in a solid. Its decay rate is determined by IMFP of signal electrons, λ_i, [42] and the cosine of the emission angle

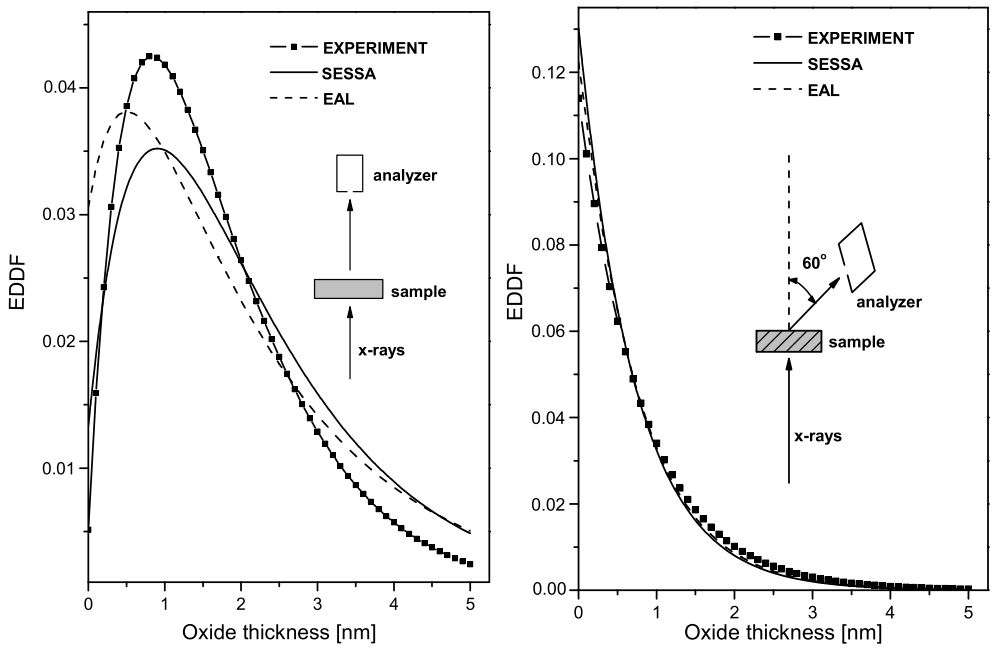

Fig. 1. The escape probability (EDDF) of O 1s photoelectrons leaving an iron oxide surface in the so-called transmission experimental geometry. (a) An X-ray incidence angle of 0° and an emission angle of 0° measured from the surface normal. (b) An X-ray incidence angle of 0° and an emission angle of 60° measured from the surface normal.

measured from the surface normal.

$$f(E,\alpha) = \exp(-z/\lambda_i \cos\alpha). \tag{3}$$

2.2 Electron elastic scattering effects

The pronounced influence of elastic scattering of signal electrons on the shape of the EDDF of the O 1s photoelectrons leaving iron oxide surface is illustrated in Fig. 1(a). The experiment was carried out in the so-called transmission geometry. The X-ray source was positioned on the opposite side of an iron foil with respect to the analyzer. The sample should be thin enough to provide good X-ray transmission and should be sufficiently thick with respect to the mean escape depth of photoelectrons leaving the upper side of the sample adjacent to the analyzer. The measured EDDF as well as those calculated by MC approach [43] and analytically [44] compare well clearly demonstrating a non-monotonic behavior of the EDDF. The EDDFs are normalized so that the $f(z,\alpha)$ satisfies the following condition:

$$\int_0^\infty f(z,\alpha) = 1, \tag{4}$$

where z is the depth measured from the sample surface. For increasing angle Θ, position of the EDDF maximum was shifted towards the surface. At Θ=60°, the EDDF can be approximated with a good accuracy by exponential (see Fig. 1(b)). However, the decay rate is determined by the total mean free path of signal electrons, λ_t,

$$\lambda = \lambda_i \lambda_{tr} / (\lambda_i + \lambda_{tr}), \tag{5}$$

where λ_{tr} is the transport mean free path [22] accounting for electron elastic scattering effects. Therefore, the SLA approach can be partially corrected for the electron elastic scattering replacing $\lambda_i$by λ_t in Eq. (3).

Another procedure correcting both the initial angular distribution and the escape probability for elastic-scattering effects have been derived by Jablonski and Powell for experimental geometries frequently used in current XPS analysis on the base of extensive MC calculations [45, 46]. In this case, two correcting parameters, Q and β_{eff}, modify the cross-sections given by Eq. (2)

$$(d\sigma/d\Omega)_{el} = Q/(\sigma_i/4\pi)\{1 - 0.25\beta_{eff}(3\cos^2\Theta - 1)\}, \tag{6}$$

where

$$\beta_{eff} = a_1 \cos^2\alpha + a_2 \cos\alpha + a_3,$$

$$Q = b_1 \cos^2\alpha + b_2 \cos\alpha + b_3.$$

Values of the fitting parameters, $a_i$and b_i, are listed for each element, the principal photoelectron lines, and for Mg and Al Kα excitation lines [46]. Index "el" denotes that the elastic scattering effects are now taken into account.

Another easy to use practical procedure is to apply a software package SESSA [43] distributed by the NIST. It enables (among lot of other possibilities) to calculate photoelectron peak intensities for the experimental geometry used accounting for both elastic and inelastic electron scattering effects.

In Fig. 2, relative Si 2p intensities, $I_{Si2p(Si)}/\{I_{Si2p(Si)} + I_{Si2p(SiO2)}\}$, are plotted against emission angles for a flat silicon sample covered by a thin silicon oxide film. The MC calculations compare well with the experimental data in the whole emission angular interval. In addition, the SLA results systematically deviate from the experiment. The SLA approach partially corrected for electron elastic scattering effects (Eqs. 3 and 5) compare well with the experiment except for oblique emission angles.

2.3 Inelastic electron surface excitations

The probability for an electron leaving the solid surface without any surface excitations is described by the surface excitation parameter, SEP, $P_S(E, \alpha)$. The SEP represents the average number of surface excitation events experienced by an electron with energy E incoming and/or leaving the surface at an angle α [47].

Within a model dielectric function, the SEP has been calculated for several metals and semiconductors by Chen [23] :

$$P_S(E, \alpha) = a_{ch} E^{-1/2} \cos^{-1}\alpha, \tag{7}$$

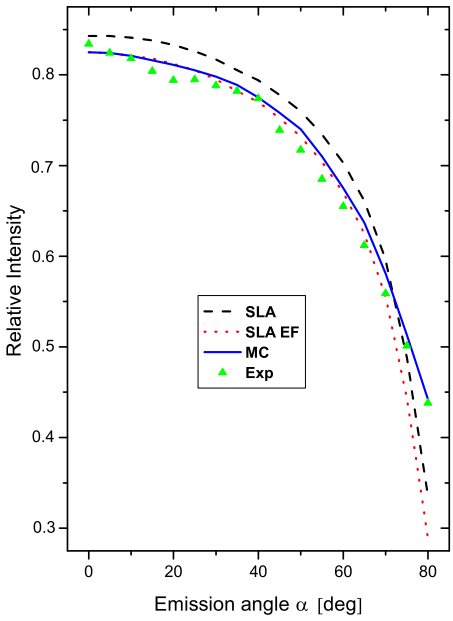

Fig. 2. Angular dependencies of relative substrate Si 2p photoelectron intensity recorded from a flat silicon sample covered by 1.1 nm of silicon oxide and by 0.5 nm of carbon contamination. Points - measurements, blue solid line - Monte Carlo calculations, black dashed line - the straight-line approximation, red dotted line - the SLA analytical calculations (partially) corrected for electron elastic scattering using Eqs. 3 and 5.

where kinetic energy E is in eV, a_{ch} is the material dependent fitting parameter.

On the base of extensive measurements of reflection energy loss spectra (REELS) for selected metals and semiconductors, Werner et al. [48] extracted the SEP values from the ratio of the number of electrons that induced a surface excitation to those elastically reflected. The SEP values have been fitted with respect to the modified Oswald‘s expression [49].

$$P_S(E,\alpha) = 1/(0.173 a_H E^{1/2} \cos\alpha + 1), \tag{8}$$

where kinetic energy E is in eV, a_H is the material dependent fitting parameter. The material parameters for 16 elements were summarized [48]. From Eqns. (7) and (8) it follows that the surface excitations are more pronounced for low kinetic energy electrons crossing a surface at oblique angles.

To overcome the lack of the SEP data, Werner et al. [48] derived a simple predictive formula to estimate the surface excitation parameter for medium energy electrons entering or leaving an arbitrary material. It is:

$$a_H/a_{HNFE} = 0.039\hbar\Omega_p + 0.4, \tag{9}$$

where Ω_p is the generalized plasmon energy and a_{HNFE} is the material parameter of nearly free

electron materials, a_{HNFE} = 0.173 eV$^{-1/2}$.

$$\Omega_p = (4\pi N N_V/m_e)^{1/2}, \tag{10}$$

where N is the atomic density, N_V is the number of valence electrons per atom, e is the elementary charge and m_e is the electron mass.

The probability for an electron incoming and leaving the solid surface without any surface excitations can be expressed [23] as $\exp[-P_S(E,\alpha)]$. Then, the X-ray photoelectron spectroscopy formalism in which elastic scattering effects have been accounted for can be extended to correct the surface effects.

$$I^s_{el} = CI_0AM(d\sigma/d\Omega)_{el}\exp[-P_S(E,\alpha)]\int_0^\infty c(z)f(E,\alpha)dz. \tag{11}$$

Here, I^s_{el} denotes given photoelectron intensity corrected for electron elastic effects as well as inelastic surface-related effects. Chen [23] has applied the above corrections on angular distributions of photoelectron intensities for several solids [50]. In addition, the procedure has been successfully used on electron elastic peak data measured for silicon [51], iron oxide [52] samples and on the Auger transition Au NOO [53].

2.4 Surface roughness

The present procedure relies on a careful surface roughness measurement by AFM. AFM patterns were evaluated by using the tilt angle histograms method (THM) [54] accounting for both true emission angles and electron shadowing. Then they were incorporated into the calculations of the angular resolved intensities by using both analytical approaches based on the straight-line approximation [1] and MC calculations with a software package SESSA [43] and finally compared with the experiment. In addition, electron elastic scattering and a surface contamination were considered. The procedure was applied and tested on angular resolved Si 2p photoelectron line intensities recorded from a flat and an artificially corrugated silicon surfaces covered with a thin silicon oxide film.

The so-called pyramid-like silicon corrugated surface is displayed in Fig. 3. Characteristic dimensions of the roughness reached several hundred nm. The surface map was converted into the histogram representation applying the THM. The THM is based on an idea that any rough surface consists of a large number of small flat areas. For all flat segments, their area, orientation and distribution were calculated, as it is illustrated in Fig. 4. In this manner, the true emission angles are properly evaluated. Also the shadowing effect was included accounting for the factual position of the electron energy analyser used. Mathematically, the procedure is rather complicated and will be published in detail elsewhere [55].

The resulted equation for total photoelectron current I_k considered in the experimental geometry k holds

$$I_k = \sum_{ij} T_{ijk} I_{ijk}, \tag{12}$$

where T_{ijk} tilt angle matrix represents the area of the sample surface that is oriented to a direction i, j and, simultaneously, is visible from the analyzer entrance slit in experimental geometry

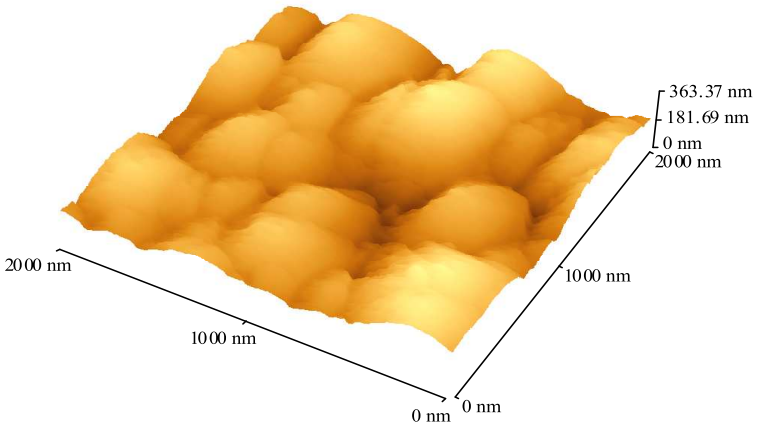

Fig. 3. AFM image of a pyramid-like corrugated silicon sample.

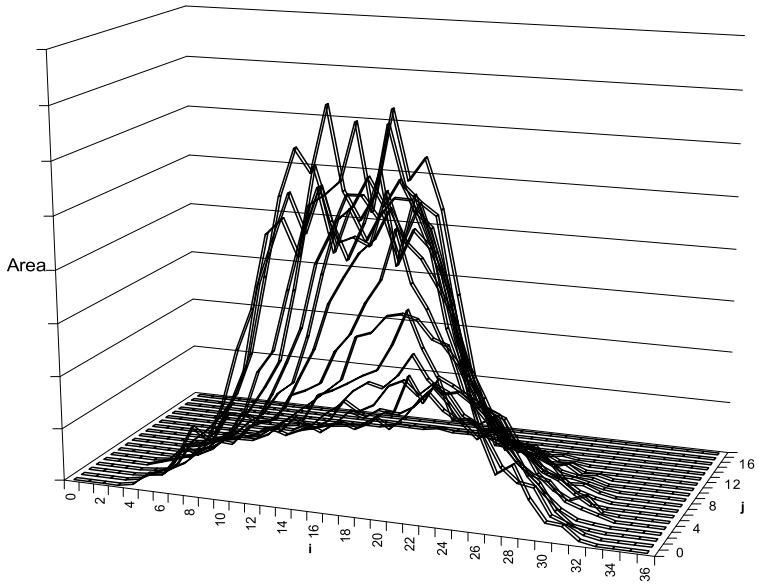

Fig. 4. Histogram of local area distributions oriented to the directions i, j for a pyramid-like corrugated silicon sample from Fig. 3.

position k. I_{ijk} is the intensity matrix. This equation completely separates the influence of surface roughness described by the tilt angle matrix T_{ijk} and the influence of depth distribution of elements below the surface incorporated in the intensity matrix I_{ijk}. Therefore, the I_{ijk} is not influenced by the surface roughness. Therefore, the I_{ijk}elements can be calculated by a

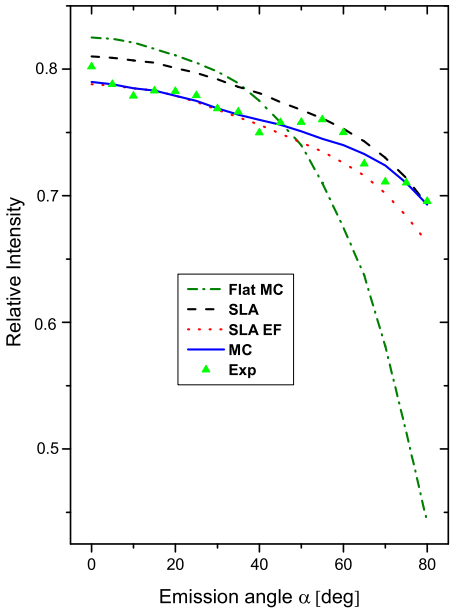

Fig. 5. Angular dependencies of relative substrate photoelectron intensity recorded from a pyramid-like silicon sample (see Fig. 3) covered by 1.1 nm of silicon oxide and by 0.5 nm of carbon contamination. Points - measurements, blue solid line - Monte Carlo calculations, black dashed line - the straight-line approximation, red dotted line - the SLA analytical calculations (partially) corrected for electron elastic scattering, green dotted - dashed line – MC calculations for a flat surface.

common procedure developed for flat samples (analytically by SLA, or SLA corrected for elastic scattering, or by MC calculations fully accounting electron inelastic and elastic scattering).

Comparison of the theory and the experiment for the silicon artificially corrugated pyramid-like surface covered by a silicon oxide film and a surface contamination overlayer is shown in Fig. 5. Here, angular dependencies of the relative substrate contribution to the Si 2p envelope calculated for the ideally flat surface, for the pyramid-like corrugated surface using the SLA approach with partial corrections for electron elastic scattering effects and using the MC calculations properly describing the electron scattering are compared with the measured data. It is clearly seen that the MC results agree well with the experiment. Contrary, large difference is evident for the data calculated under the assumption of the flat surface.

3 Summary and concluding remarks

Recent progress in understanding of electron transport at solid surfaces has led to improved reliability and precision of resulted quantitative information. As a consequence, several approximate procedures to correct effects of electron elastic scattering, surface-related inelastic events and surface roughness have been developed. In the present contribution, effects of electron elas-

tic scattering, inelastic surface excitations of signal electrons, and surface roughness are briefly reviewed with the following conclusions.

(i) Corrections for electron elastic scattering effects and full description of electron scattering accounting for elastic as well as inelastic (bulk) scattering are at present well-established and easy to use methods of quantitative analysis.

(ii) Apart from first attempts to correct electron surface excitations described in the present work, description of surface-specific inelastic interaction of signal electrons is still in its infancy. More theoretical works in the field and reliable experiments are needed.

(iii) At present, there is no easy to use method how to correct surface roughness effects. The procedure accounting for the surface corrugation is rather complicated. We present a semi empirical procedure based on a careful AFM surface mapping and tilt angle histograms. In this manner, the surface roughness effects (true emission angles and electron shadowing) are completely separated from the influence of depth distribution of elements below the surface incorporated in the intensity matrix. Therefore, the intensity matrix can be calculated in a relatively easy way by a common procedure developed for the ideally flat sample surfaces.

Acknowledgement: This work was supported by the project "Electron Transport Processes near Solid Surfaces" of Grant Agency of the Czech Republic No. 202/02/237 and the Institutional Research Plan No. AV0Z 10100521.

References

[1] C.S. Fadley, R.J. Baird, W. Sickhaus, T. Novakov, S.A. Bergstrom: *J. Electron Spectrosc. Relat Phenom.* **4** (1974) 93

[2] O.A. Baschenko, V.I. Nefedov: *J. Electron Spectrosc. Relat. Phenom.* **17** (1979) 405

[3] I.S. Tilinin, W.S.M. Werner: *Phys. Rev. B* **46** (1992) 13739

[4] A. Jablonski, J. Zemek: *Phys. Rev. B* **48** (1993) 4799

[5] V.M. Dwyer: *Surf. Sci.* **310** (1994) L621

[6] V.I. Nefedov: *J. Electron Spectrosc. Relat. Phenom.* **100** (1999) 1

[7] A. Jablonski, S. Tougaard: *Surf. Sci.* **432** (1999) 211

[8] A. Jablonski, I.S. Tilinin, C.J. Powell: *Phys. Rev. B* **54** (1996) 10927

[9] A. Jablonski, H. Ebel: *Surf. Interface Anal.* **11** (1988) 627

[10] S. Hucek, J. Zemek, A. Jablonski: *J. Electron Spectrosc. Relat. Phenom.* **85** (1997) 257

[11] A. Jablonski, C.J. Powell: *Phys. Rev. B* **50** (1994) 4739

[12] I. S. Tilinin, A. Jablonski, J. Zemek, S. Hucek: *J. Electron Spectrosc. Relat. Phenom.* **87** (1997) 127

[13] I. S. Tilinin, A. Jablonski, W. S. M. Werner: *Prog. Surf. Sci.* **52** (1996) 193

[14] W.H. Gries, W.S.M. Werner: *Surf. Interface Anal.* **16** (1990) 149

[15] A. Jablonski, S. Tougaard: *J. Vac. Sci. Technol. A* **8** (1990) 106

[16] J. Zemek, S. Hucek, A. Jablonski, I.S. Tilinin: *Surf. Interface Anal.* **26** (1998) 182

[17] J. Zemek, P. Jiricek, S. Hucek, A. Jablonski, B. Lesiak: *Surf. Sci.* **473** (2001) 8

[18] J. Zemek, P. Jiricek, S. Hucek, B. Lesiak, A. Jablonski: *Surf. Interface Anal.* **30** (2000) 222
[19] J. Zemek, S. Hucek: *Fresinius J. Anal. Chem.* **363** (1999) 156
[20] S. Hucek, J. Zemek, A. Jablonski, I.S. Tilinin: *Surf. Rev. Lett.* **7** (2000) 109
[21] J. Zemek, P. Jiricek, K. Olejnik: *Surf. Sci.* **572** (2004) 93
[22] *Surface Analysis by Auger and X-Ray Photoelectron Spectroscopy, D. Briggs, J.T. Grant.* Eds., IM Publications and Surface Spectra Limited, 2003
[23] Y.F. Chen: *Surf. Sci.* **519** (2002) 115
[24] R.H. Ritchie: *Phys. Rev.* **106** (1957) 874
[25] E.A. Stern, R.A. Ferrell: *Phys. Rev.* **120** (1960) 130
[26] P. Echenique, J. Pendry: *J. Phys. C: Solid State Phys.* **8** (1975) 2936
[27] F. Yubero, S. Tougaard *Phys. Rev. B* **46** (1992) 2486
[28] C.J. Tung, Y.F. Chen, C.M. Kwei, T.L. Chou: *Phys. Rev. B* **49** (1994) 16684
[29] M. Vicanek *Surf. Sci.* **400** (1999) 1
[30] K.L. Aminov, J.B. Pederson: *Phys. Rev.* **63** (2001) 125412
[31] Y.F. Chen: *Surf. Sci.* **345** (1996) 213
[32] W.S.M. Werner: *Surf. Interface Anal.* **23** (1995) 696
[33] O.K.T. Wu, G.G. Peterson, W.J. LaROCCA, E.M. Butler: *Appl. Surf. Sci.* **11/12** (1982) 118
[34] M.F. Ebel, G. Moser, H. Ebel, A. Jablonski, H. Oppolzer: *J. Electron Spectrosc. Relat. Phenom.* **42** (1987) 61
[35] P.L.J. Gunter, J.W. Niemantsverdriet: *Appl. Surf. Sci.* **89** (1995) 69
[36] P.L.J. Gunter, O.L.J. Gijzeman, J.W. Niemantsverdriet: *Appl. Surf. Sci.* **115** (1997) 342
[37] R.C. Chatelier, H.A.W. St John, T.R. Gengenbach, P.Kingshott, H.J. Griesser: *Surf. Interface Anal.* **25** (1997) 741
[38] K. Vutova, G. Mladenov, T. Tanaka, K. Kawabata: *Surf. Interface Anal.* **30** (2000) 552
[39] K. Vutova, G. Mladenov, T. Tanaka, K. Kawabata: *Vacuum* **62** (2001) 297
[40] J.W. Cooper, S.T. Manson: *Phys. Rev.* **177** (1969) 157
[41] *ASTM Standards E673-95, Annual Book of ASTM Standards*, American Society for Testing and Materials, West Conshohocken, PA, Vol. 3.06, 1997, p.907
[42] C.J. Powell, A. Jablonski: *J. Phys. Chem. Ref. Data* **28** (1999) 19
[43] W.S.M. Werner, W. Smekal, C.J. Powell: *Simulation of Electron Spectra for Surface Analysis (SESSA) – Version 1.0β1*, National Institute of Standards and Technology, Gaithersburg, MD (2003)
[44] C.J. Powell, A. Jablonski: *NIST Electron Effective-Attenuation-Length Database*, Standard Reference Database 82, National Institute of Standards and Technology
[45] A. Jablonski, C.J. Powell: *Surf. Interface Anal.* **20** (1993) 771
[46] A. Jablonski: *Surf. Interface Anal.* **23** (1995) 29
[47] R.F. Egerton: *Electron Energy-Loss Spectroscopy in the Electron Microscope*, Plenum Press, New York, 1986
[48] W.S.M. Werner, W. Smekal, C. Tomastik, H. Stori: *Surf. Sci.* **486** (2001) L461
[49] R. Oswald: *Ph.D. Thesis*, Eberhard-Karls-Universitat Tubingen, 1992
[50] S. Hucek, I.S. Tilinin, J. Zemek: *J. Electron Spectrosc. Relat. Phenom.* **85** (1997) 263
[51] J. Zemek, P. Jiricek, B. Lesiak, A. Jablonski: *Surf. Sci.* **562** (2004) 92
[52] B. Lesiak, A. Jablonski, J. Zemek, P. Jiricek, M. Cernansky: *Appl. Surf. Sci.* **36** (2004) 816
[53] A. Jablonski, J. Zemek, P. Jiricek: *Appl. Surf. Sci.* (2005) in print
[54] K. Olejnik: *Diploma thesis* MFF UK, Praha 2004
[55] K. Olejnik, J. Zemek, W. S.M. Werner: *Surf. Sci.*, submitted for puiblication